Journal of Solar Energy Research (JSER)

Journal homepage: www.jser.ut.ac.ir

Design Output Control TLB Converter for DC Drive Applications with photovoltaic power supply

Mohammadreza Samadi[a,*], Seyed Mehdi Rakhtala[b]

[a] *Faculty of Electrical and Computer Engineering, Noshirvani University of Technology, Babol, Iran E-mail: samadi_6947@yahoo.com*
[b] *Faculty of Electrical Engineering, Golestan University, Gorgan, Iran*

ARTICLE INFO

Received:31 Aug 2017
Received in revised form: 14 Sept 2017
Accepted: 25 Sept 201
Available online: 05 Oct 2017

Keywords:
photovoltaic, Internal generated voltage**,** TLB converter, voltage-balancing control, PI controller

A B S T R A C T

Using conventional boost converter in photovoltaic system as the interface between the photovoltaic panel and the consumer is widely practiced. In this paper, instead of using conventional boost converter, the three-level boost converter (TLBC) has been used. The advantages of TL converters include reduced voltage stress of the switches, reduced filter size, and improved dynamic response. However, the capacitor voltages may be different due to their mismatched equivalent series resistance, their mismatched capacitance, and the mismatched conducting time of the corresponding switches. This paper investigates the output control TLB converter for dc drive applications. A PI controller method is applied for adjusting the output voltage and internal generated voltage . That Kp and Ki gains set as well and output is very smooth and free of oscillation generated. On the other hand, the voltage can be controlled to transmit dc motor. A P controller method is then used for the individual capacitors voltage balancing. At the absence of control, voltage capacitors are also many differences. Simulation results show the high dynamic performance of the controller in adjusting the capacitors' voltages and output control TLB converter.

1. Introduction

The three-level boost-type converters shown in Fig. 1 have the advantages of the low voltage stress, the low inductor current ripple and the low switching loss [12]. The idea of having circuits that generate three-level (TL) voltage waveforms can be traced back to two U.S. patents granted in the early 1960s [3], [4]. These TL circuits were invented for computer applications with the intention of transforming conventional computation methodology from binary logic form to ternary form. Later, Nabae *et al.* [5] and Baker1 [6] reported a different form of TL circuits specific to power conversion application in 1980 and 1981, respectively. The circuit is named the neutral-point-clamped (NPC) inverter. In contrast to conventional power inverter, the phase leg of this inverter can but also the neutral-point voltage. As a result, the output voltage of the NPC inverter has lower harmonics as compared to that of traditional inverters [7]. This allows the use of a smaller output filter. Since the phase leg provides three levels of voltages, the NPC inverter is also called TL inverter. An additional advantage of the TL inverter is that the voltage stress of the switches is reduced to half of the input voltage, which makes it suitable for high input voltage power conversions [8]. This technique has been applied to dc–dc converters by Pinheiro and Barbi [9], [10] to reduce the voltage stress of the switches. The recent increase in the interfacing of renewable energy inverters are turn out to be the inevitable appliance for power conversion. The multilevel converter provides advantages such as lower harmonic distortion and reduction in dV/dt of the output voltage. The three-level boost (TLB)

converter has several advantages in high voltage applications such as reduced switching losses and lower reverse recovery losses of the diode [11]–[13] compared to the conventional boost converters. In [11], [12], [14] the circuit is employed and studied with a different approach for power factor correction by controlling the duty ratio of the switches. The maximum power point tracking by direct duty ratio control of TLB converter using a power hysteresis is presented in [13]. Independent control of TLB switches for balancing of dc-link capacitors is discussed in [15]. In [16] the SSPDC method is proposed for TLB circuit to balance the neutral point voltage with simulation results. Additionally, the paper considers only the three modes of operation of TLB.

This paper propose output control TLB converter for dc drive applications Using photovoltaic module as the input power supply. A PI controller method is applied for adjusting the output and internal generated voltage. A P controller method is then used for the individual capacitors voltage balancing.

The system, with a simple proportional-integral controller will be able to deliver any voltage to the output of the engine. In addition, if voltage balancing control is not done, Causing damage to the equipment and the engine characteristic.

Finally, Simulation results show the high dynamic performance of the controller in adjusting the capacitors' voltages and output control TLB converter.

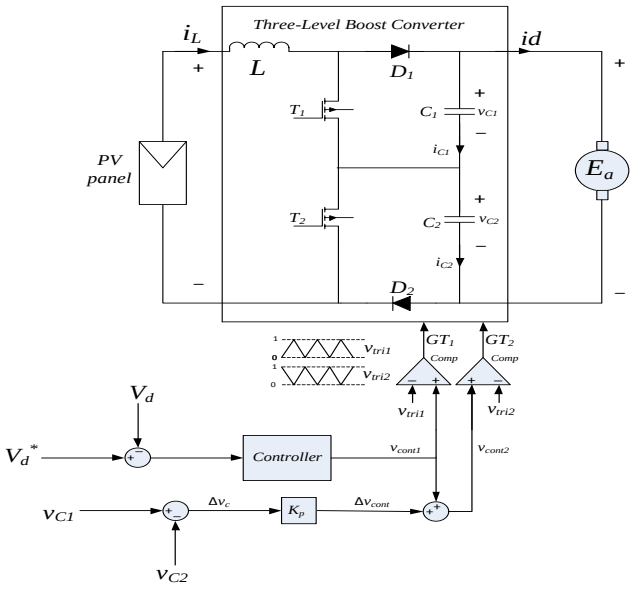

Figure 1.TLB converter with its capacitor voltage balancing control loop.

2. Material and Methods

2.1. PV Panel Modeling

The equivalent circuitry of a PV cell is shown in Fig. 2, in which the simplest model can be represented by a current source in antiparallel with a diode. The nonidealities are represented by the insertion of the resistances *Rs* (series resistance) and *Rp* (parallel resistance).

The PV panel simulation model is based on the output current of one PV equivalent model, and its mathematical equation is represented by:

$$I = I_{ph} - I_r \cdot \left[e^{q.\frac{V+I.R_S}{\eta.k.T}} - 1 \right] - \frac{V + I.R_S}{R_P} \quad (1)$$

where V represents the output PV voltage of one PV panel, I_{ph} is the photocurrent, I_r is the saturation current, q is the electrical charge (1.6×10^{-19} C), η is the p-n junction quality factor, k is the Boltzmann constant (1.38×10^{-23} J/K), and T is the temperature (in kelvins).

Equation (1) can be modified in order to present a null root when current I approaches the real PV current. So, (1) is rewritten (2) as a function of its own PV current

$$f(I) = I_{ph} - I - I_r \cdot \left[e^{q.\frac{V+I.R_S}{\eta.k.T}} - 1 \right] - \frac{V + I.R_S}{R_P} \quad (2)$$

Current I, with a null initial value, is utilized in an iterative process that approximates (2) of its root, being obtained by the Newton–Rhapson method (3), which seeks the zero of the differentiable function

$$x_{n+1} = x_n - \frac{f(x_n)}{f'(x_n)} \quad (3)$$

Thus, the derivative of (2) is presented in

$$f(I) = -1 - I_r \cdot \left[e^{q.\frac{V+I.R_S}{\eta.k.T}} \right] \frac{q.R_S}{\eta.k.T} - \frac{R_S}{R_P} \quad (4)$$

With the aforementioned equations, an embedded function to simulate a typical PV panel in MatLab/Simulink was created.

The model was used as a voltage source, and the integrator represents the capacitance that stores the injected current from the PV panel. The PV electrical parameters are presented in Table 1.

Figs 3-6, show the I-V and P-V characteristics of a typical PV module in different of temperatures and solar irradiance levels.

The curves show clearly the nonlinear characteristics, and they are strongly influenced by climate changes.

Table1. ELECTRICAL PARAMETERS OF THE PV CELL

Maximum Power	$\mathbf{P_{MAX}}$=*83.1W*
Voltage at MPP	$\mathbf{V_{MPP}}$=*17.15V*
Current at MPP	$\mathbf{I_{MPP}}$=*4.85A*
Open Circuit Voltage	$\mathbf{V_{OC}}$=*21.2V*

Short Circuit Current	$\mathbf{I_{SC}}$=*5.27A*
Temperature Coefficient of $\mathbf{I_{sc}}$	$\boldsymbol{\alpha}$=*0.65*10^{-3}A/^{o}C*

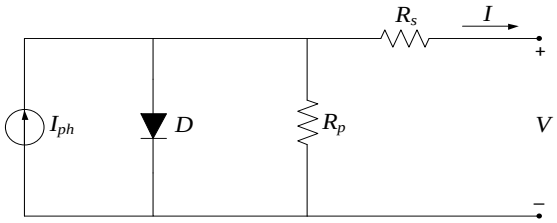

Figure2. Equivalent model of the PV panel

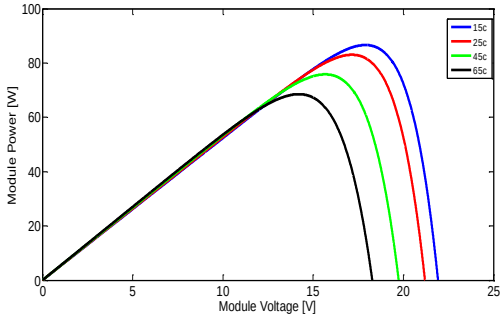

Figure3. P-V characteristics of a typical PV module for varied Temperatures.

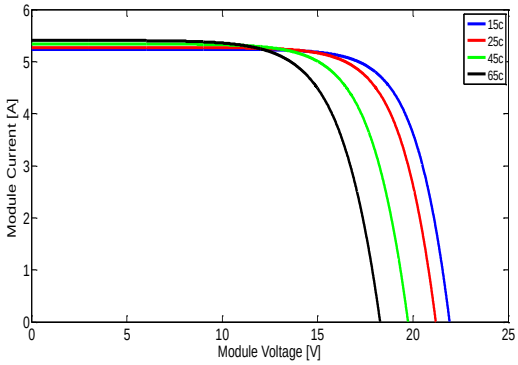

Figure4. I-V characteristics of a typical PV module for varied Temperatures.

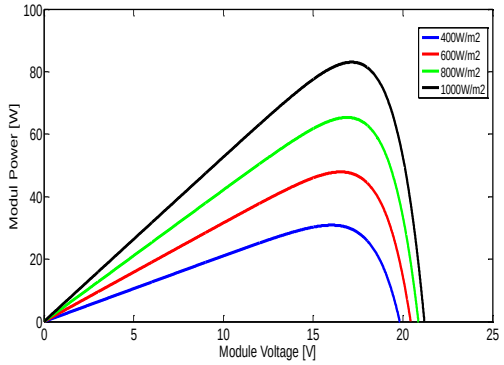

Figure5. P-V characteristics of a typical PV module for varied solar irradiances.

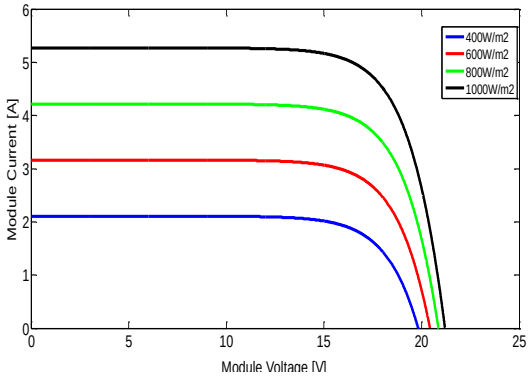

Figure6. I-V characteristics of a typical PV module for varied solar Irradiances.

2.2. Characteristic of DC Motor

The characteristic of a DC motor is govern by equation (5) :

$$E_a = V_A - I_a R_a \quad (5)$$

where *VA* is the applied voltage across the DC motor, *Ia* is the armature current, *Ra* is the armature resistance and E_a is the internal generated voltage. In normal operating condition, the armature current will increase with the applied voltage and the internal generated voltage remains constant. Turning speed of motor is directly proportional with internal generated voltage, showing in the equation (6):

$$E_a = K\phi\omega \quad (6)$$

Where ø is magnetic flux, ω is the turning speed of DC motor and *K* is a constant. Here the armature current is the same as the output current of the TLB convertor.

2.3. TLB Converter

Fig. 1. shows the TLB along with its control circuit. By assuming that the switching frequency *fs* is much larger than the line frequency *f*, the control signals v_{cont1} and v_{cont2} can be regarded as two constants within the switching period *Ts* = 1/*fs* . In addition, the ideal inductor and the ideal capacitors are assumed. That is, the inductor resistance and the Capacitors' resistances are assumed to be zero.

According to this figure, two triangular signals v_{tri1} and v_{tri2} are interleaved by 180◦ .The conventional PI control generates the control signal v_{cont1}, and then, the gate signalGT_1 is generated from the comparison of the control signal v_{cont1} and the triangular signal v_{tri1} .

After sensing both capacitor voltages, the voltage imbalance is detected and the conventional capacitor voltage balancing control (CVBC) generates the compensation signal Δv_{cont}. Then, the other control signal v_{cont2} is obtained by adding the compensation

signal Δv_{cont} to the control signal v_{cont1}. The gate signal GT_2 is obtained from the comparison of the control signal v_{cont2} and the triangular signals v_{tri2} .

Due to the input inductor L and two diodes D_1 and D_2 in the TLB converter, both switches can be conducting at the same time without the concern of the short circuit damage. As plotted in Fig. 7, there are four switching states in the TLB converter.

As shown in Fig. 7(a), both switches are turned on in the switching state 1. Thus, the inductor voltage V_L in the TLB converter equals the input voltage $V_L = V_{pv}$ and both capacitors supply energy to the load $i_{C1} = i_{C2} = (-i_d) < 0$.

In the switching state 2 in Fig. 7(b), the top switch turns on and the bottom switch turns off. The resulting inductor voltage V_L equals the input voltage V_{pv} minus the bottom capacitor voltage $V_L = V_{pv} - V_{C2}$. Additionally, the capacitor C_1 supplies energy to the load $i_{C1} = (-i_d) < 0$, but the capacitor C_2 stores the energy from the input voltage $i_{C2} = (i_L - i_d) > 0$. Similarly, the resulting inductor voltage in Fig. 7(c) equals the input voltage minus the top capacitor voltage $V_L = V_{pv} - V_{C1}$. In the switching state 3, the top capacitor C_1 is charged $i_{C1} = (i_L - i_d) > 0$, but the bottom capacitor C_2 is discharged $i_{C2} = (-i_d) < 0$.

When both switches turn off in Fig. 7(d), the resulting inductor voltage equals the input voltage minus the output voltage $V_L = V_{pv} - E_a = V_{pv} - v_{C1} - v_{C2}$. The input voltage V_{pv} supplies the load current and charges both capacitors simultaneously $i_{C1} = i_{C2} = (i_L - i_d) > 0$. All the capacitor currents in various switching states are tabulated in Table 2.

The behavior of the TLB converter can be divided into two cases as shown in Fig. 8. In the case of $2 > v_{cont1} + v_{cont2} > 1$, two switches may conduct at the same time within the switching period Ts and there are switching state 1, state 2, and state 3.

In the other case of $1 > v_{cont1} + v_{cont2} > 0$, only switching state 2, state 3, and state 4 exist. In the case of $2 > v_{cont1} + v_{cont2} > 1$ in Fig. 8(a), the conducting times of the switching state 2 and the switching state 3 are $(1 - v_{cont2})Ts$ and $(1 - v_{cont1})Ts$, respectively. The remaining time for the switching state 1 is $(v_{cont1} + v_{cont2} - 1)Ts$. Similarly, for the other case of $1 > v_{cont1} + v_{cont2} > 0$ in Fig. 8(b), the conducting times of the switching state 2 and state 3 are $v_{cont1}\ Ts$ and $v_{cont2}\ Ts$, respectively. The remaining time for the switching state 4 is $(1 - v_{cont1} - v_{cont2})Ts$.

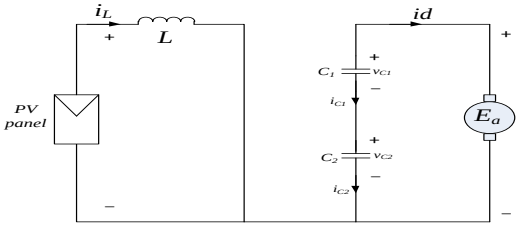

(a)

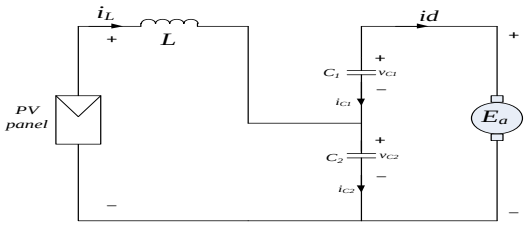

(b)

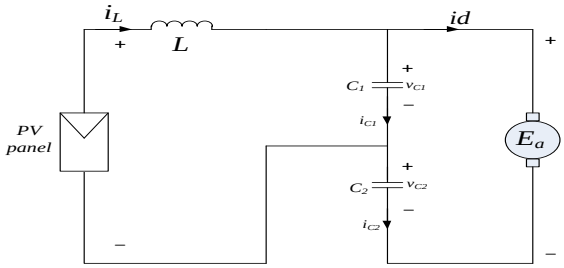

(c)

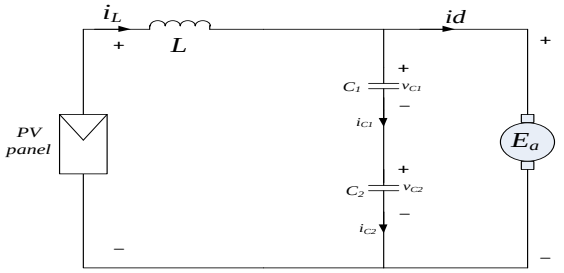

(d)

Figure7. Possible switching states in the TLB converter: (a) state 1, (b) state 2, (c) state 3, and (d) state 4.

Table2. CAPACITOR CURRENTS IN EACH STATE

		State 1	State 2	State 3	State 4
$1<v_{cont1}+v_{cont2}<2$	i_{C1}	$-i_O < (0)$	$-i_O < (0)$	$i_L-i_O > (0)$	
	i_{C2}	$-i_O < (0)$	$i_L-i_O > (0)$	$-i_O < (0)$	
$0<v_{cont1}+v_{cont2}<1$	i_{C1}		$-i_O < (0)$	$i_L-i_O > (0)$	$i_L-i_O > (0)$
	i_{C2}		$i_L-i_O > (0)$	$-i_O < (0)$	$i_L-i_O > (0)$

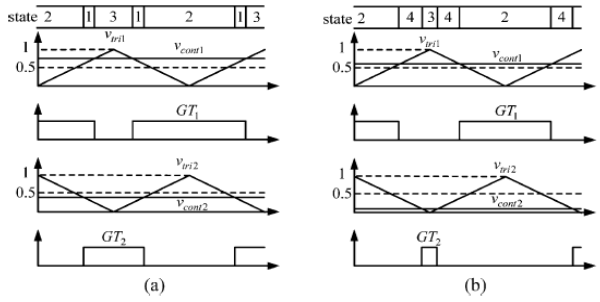

Figure8. Behavior of the TLB converter. (a) 2 > v_{cont1} + v_{cont2} > 1and (b) 1 > v_{cont1} + v_{cont2} > 0.

2.4. Capacitor Voltage Balancing Control

In the TLB converter shown in Fig.1, an outer control loop with P controller is used to balance the two capacitors voltages. The controller output is added with *v*cont1 so as to both balance the capacitors' voltages and makes Δ*v*cont zero to equalize the rate of v_{cont1} and v_{cont2}. Without this control loop the individual capacitor voltage balancing will be lost and an unbalanced condition will occur in the output voltage at the network side.

It follows that the voltage imbalance $\Delta v_C = v_{C1} - v_{C2}$ can be expressed as :

$$\Delta v_C = \frac{1}{S}\frac{\Delta v_{cont}}{C} i_L \qquad (7)$$

where $\Delta v_{cont} = v_{cont2} - v_{cont1}$.

The equivalent voltage balancing loop with the conventional CVBC is plotted in Fig. 9 where the proportional controller (i.e., P controller) with the parameter *KP* is used. Thus, the closed-loop transfer function of the voltage imbalance Δ*vC* (*s*) becomes

$$\frac{\Delta v_C(s)}{\Delta v_C^*(s)} = \frac{\frac{K_P}{C} i_L}{S + \frac{K_P}{C} i_L} \qquad (8)$$

As equation (8) is a first-order response with zero steady state error, the voltage imbalance would be well regulated to zero ($\Delta v_C^* = 0$). Therefore, the design of the conventional CVBC with simple P controller is able to balance the capacitor voltages.

3. Simulation results

In this section, the simulation results of the TLB converter are provided. System parameters are tabulated in Table 3. the capacitance-mismatch condition are helpful for the demonstration of the proposed CVBC.

Fig. 10. shows the output voltage of 89V. As can be seen in the figure it reaches the steady state condition in 0.02 seconds and delivers a smooth output to the net. If the DC motor demands different voltages, it can achieve totally controlled voltages. The balanced capacitors' voltages have also been shown in Fig. 11.

Fig. 12 and 13 show the absence and presence of CVBC proposed for capacitor voltages. Fig. 12 shows the inequality of the voltages when CVBC is separated from the circuit. The capacitors' voltages are completely separate and unequal. Fig. 13 shows magnify the voltage waveforms in the presence of CVBC.

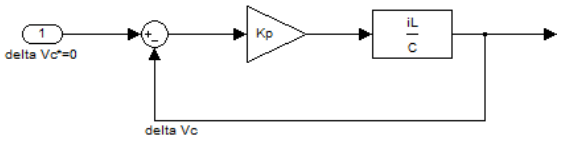

Figure9. Equivalent voltage balancing loop with the conventional CVBC.

Table3. SIMULATED PARAMETERS OF TLB CONVERTER

Input voltage	17.15V
Output voltage	89V
Inductor	75µH
Carrier frequency	10KHz
Capacitor	C_1=400µF, C_2=420µF
Voltage balance parameter	K_P=0.03
Output voltage parameter	K_{PV}=0.2 ,K_{iV} =0.001
Resistance	200 Ohm

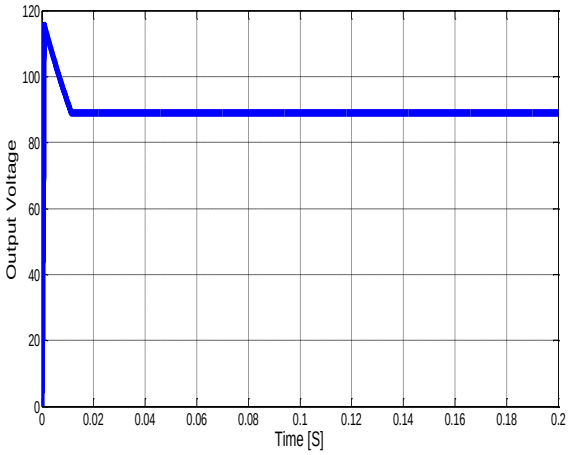

Figure10. Simulation result for the TLB converter at 89v.

4. Conclusion

In this paper, A PI controller method is applied for adjusting the output and internal generated voltage. Also, the CVBC method for the TLB converter has been proposed. This method, generally, is conducted

in a complete controlled way for all output voltage levels, and for all levels, the capacitor voltage balancing is correctly done and can be delivered to the network or any other applications as second quadrant energy regeneration system in electric vehicle. simulation results show the high dynamic performance of the controller in adjusting the capacitors' voltages and output control TLB converter.

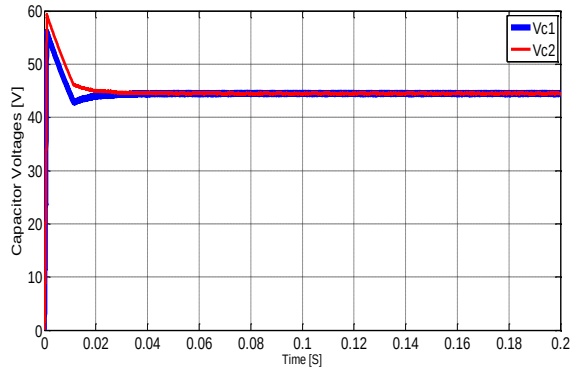

Figure11. Capacitor voltage balance

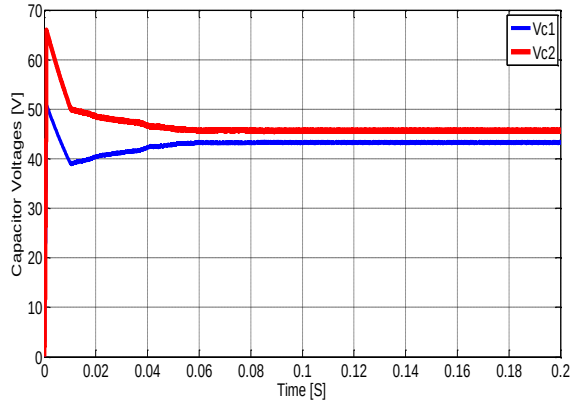

Figure12. Capacitor voltages without CVB

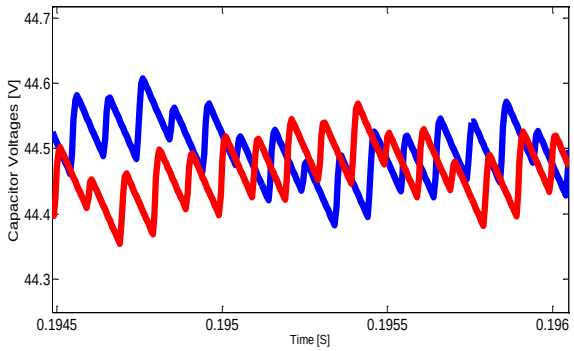

Figure13. Capacitor voltages are magnified by CVBC

References

[1] M. T. Zhang, Y. Jiang, F. C. Lee, and M. M. Jovanovic, "Singlephase three-level boost power factor correction converter," in *IEEE APEC,95*, pp. 434-439, 1995.

[2] H. Wu and X. He, "Single Phase Three-Level Power Factor Correction Circuit with Passive Lossless Snubber" *IEEE Trans. Power Electronics*, vol. 17, no. 6, pp. 946-953, Nov. 2002.

[3] K. M. Trampel, "Three-level inverter circuit," U.S. Patent 3 060 330,Oct. 23, 1962.

[4] A. J. Gruodis, L. K. Lange, and W. H. Mcanney, "Three level converter,"U.S. Patent 3 155 845, Nov. 3, 1964.

[5] A. Nabae, I. Takahashi, and H. Akagi, "A new neutral-clamped PWM inverter," in *Conf. Rec. IEEE IAS Annu. Meeting*, 1980, pp. 761–766. [6] R. H. Baker, "Bridge converter circuit," U.S. Patent 4 270 163, May 26, 1981. [7] D. Czarkowski, D. V. Chudnovsky, G. V. Chudnosky, and I. W. Selesnick, "Solving the optimal PWM problem for single-phase inverters," *IEEE Trans. Circuits Syst. I, Fundam. Theory Appl.*, vol. 49, no. 4, pp. 465–475, Apr. 2002. [8] E. E. H. Ismail, M. M. A. Al-Saffar, and A. A. J. Sabzali,"Highconversion ratio DC–DC converters with reduced switch stress," *IEEETrans.CircuitsSyst. I, Reg. Papers*, vol. 55, no. 7, pp. 2139–2151, Aug. 2008. [9] J. R. Pinheiro and I. Barbi, "The three-level ZVS PWM converter—A new concept in high-voltage DC-to-DC conversion," in *Proc. IEEE IECON*, 1992, pp.173-178. [10] J. R. Pinheiro and I. Barbi, "Wide load range three-level ZVS-PWM DC-to-DC converter," in *Proc. IEEE PESC*, 1993, pp. 171–177. [11] G. Yao, M. Ma, Y. Deng, W. Li, and X. He, "An improved ZVT PWM three level boost converter for power factor preregulator",Power Electronics Specialists Conference, 2007. PESC 2007. IEEE , vol., no.,pp.768-772, June 2007.

[12] M. T. Zhang, J. Yimin, F. C. Lee, and M. M. Jovanovic, "Single-phaseTLB power factor correction converter," in Proc. of IEEE APEC '95 Conf., 1995, pp. 434-439 vol.1.

[13] J-M. Kwon, B-H. Kwon, and K-H. Nam, "Three-phase photovoltaic system with TLBing mppt control",IEEE Tran. on Pow. Elec., vol. 23, no. 5, pp.2319-2327, Sep. 2008.

[14] J. R. Pinheiro, D. L. R. Vidor, and H. A. Grundling, "Dual output threelevel boost power factor correction converter with unbalanced loads",Conf. Rec. IEEE PESC',96, pp.733 -739 1996

[15] V. Yaramasu, B. Wu, "Three Level Boost Converter based Medium Voltage Megawatt PMSG Wind Energy Conversion Systems", 3 rd IEEEEnergy Conversion Congress and Exposition (ECCE), pp. 561-567, Sep. 2011.

[16] Xia, C.L.; Gu, X.; Shi, T.N.; Yan, Y. "Neutral-Point potential balancing of three-level inverters in direct-driven wind energy conversion system". IEEE Transactions on Energy Conversion , vol.26, No. 1, 18-29,2011